ELSEVIER

Journal of Organometallic Chemistry 634 (2001) 136–144

Journal of Organometallic Chemistry

www.elsevier.com/locate/jorganchem

EPR and theoretical studies of the reduction product of the fulvenephosphaallene system

M. Chentit [a], H. Sidorenkova [a], S. Choua [a], M. Geoffroy [a,*], Y. Ellinger [b,*], G. Bernardinelli [c]

[a] *Department of Physical Chemistry, University of Geneva, 30 quai E. Ansermet, 1211, Geneva, Switzerland*
[b] *Laboratoire d'Etude Théorique des Milieux Extrèmes, Université de Nice-Sophia Antipolis et Observatoire de la Côte d'Azur, 06108 Nice, France*
[c] *Laboratory of Crystallography, University of Geneva, 24 quai E. Ansermet, 1211, Geneva, Switzerland*

Received 15 May 2001; accepted 5 July 2001

Abstract

Fluoren-9-ylidenemethylene-(2,4,6-tri-*tert*-butyl-phenyl)phosphane (**2**), a new type of phosphaallene with the terminal carbone incorporated in a cyclopentadienyl ring, has been synthesized and its crystal structure has been determined. The ^{31}P and ^{13}C (central carbon) hyperfine tensors of the reduction compound of this phosphaallene have been measured on the EPR spectra recorded after electrochemical reduction of a solution of **2** in THF. Structures of the model molecules HP=C=Cp (where Cp is a cyclopentadienyl ring), $[HP{=}C{=}Cp]^{\bullet -}$ and $[HP{-}CH{=}Cp]^{\bullet}$ have been optimized by DFT and the hyperfine couplings of the paramagnetic species have been calculated by DFT and SCI methods. The comparison between the experimental and the theoretical results shows that, in solution, the radical anion $[\mathbf{2}]^{\bullet -}$ is readily protonated and that the EPR spectra are due to the phosphaallylic radical. © 2001 Published by Elsevier Science B.V.

Keywords: Phosphaallenes; EPR; DFT; Radical anion; Phosphaallylic radical

1. Introduction

Unsaturated systems containing one or more low-coordinated phosphorus atoms possess low energy antibonding π orbitals [1] which confer interesting electron transfer properties to these types of molecules. It is well established that chemical or electrochemical reduction of a P=C [2] or a P=P [3] double bond leads to the formation of a rather persistent radical monoanion. In the case of phosphaallenes [4] the presence of two adjacent orthogonal π-systems makes the identification of the reduction product less straightforward. Contrary to a first interpretation of the EPR spectrum obtained after reduction of ArP=C=PAr [5], it seems that the basicity of the radical anion is so high, that the species observed by EPR corresponds to the phosphaallylic radical [6]. A phosphaallylic species was indeed obtained after reduction of $ArP{=}C{=}CPh_2$ [7]. Differentiation between the radical monoanion and the allylic species is made difficult by the fact that the hyperfine splitting with the additional proton is expected to be small and can remain unresolved for molecules with a large rotational correlation time. Since low-coordinated trivalent phosphorus needs to be protected by a bulky group [8,9] (e.g. the tri-*tert*-butyl phenyl Ar) the linewidths of the corresponding EPR signals are generally large, and the identification of the reduction product depends only on the interpretation of the ^{31}P and ^{13}C hyperfine couplings. This interpretation requires the knowledge of the electronic configuration of both the anionic and neutral species and, consequently, provides the incentive to investigate these two systems by quantum mechanical calculations.

The objective of this study is to determine to what extent the presence of a cyclopentadiene ring (Cp) is able to affect the structure of the reduction product of a phosphaallenic molecule. The high stability of the cyclopentadienide anion is expected to favor the separation between spin and negative charge, and explains, for example, the drastic increase in the phosphorus

* Corresponding authors.

0022-328X/01/$ - see front matter © 2001 Published by Elsevier Science B.V.
PII: S0022-328X(01)01098-1

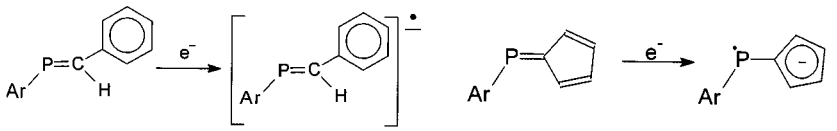

Scheme 1.

coupling constant (from $A_{iso} = 152$ to 252 MHz) which accompanies the replacement of a phenyl methylene moiety by a cyclopentadienyl ring in a phosphaalkene radical anion [10] (Scheme 1).

For the phosphaallene **1** the same mechanism (Scheme 2) would formally give the vinylic type radical **1a** and, therefore, lead to a low phosphorus spin density. However, according to previous observations on ArP=C=CPh$_2$ [7], it is also possible that reduction of **1** leads to the phosphaallylic radical **1b**.

In order to assess the behavior of this particular system when subject to reduction, we decided to synthesize a new type of phosphaallene whose terminal carbon atom is incorporated in a cyclopentadiene ring. We report here the preparation of fluoren-9-ylidenemethylene-(2,4,6-tri-*tert*-butyl-phenyl)phosphane **2** and of the ^{13}C-enriched compound **2**(^{13}C) as well as its crystal structure. Information on the reduction of **2** is obtained from liquid/frozen solution EPR together with ab initio/DFT calculations on the representative model systems **3**.

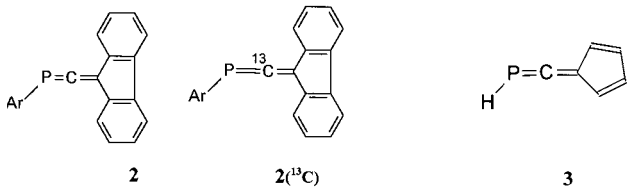

2 **2**(^{13}C) **3**

Ar = 2,4,6-tri-tert-butyl-phenyl

2. Materials and methods

2.1. Synthesis

Compound **2** was synthesized by following a method similar to that used by Yoshifuji et al. for the synthesis of ArP=C=CPh$_2$ [11]. ^{t}BuLi (1.44 ml, 1.5 M in hexane) was added dropwise, at −78 °C, to a solution of ArP=C(Cl)SiMe$_3$ (245 mg) in 15 ml THF. (ArP=C(Cl)SiMe$_3$ was prepared by successive additions of ^{n}BuLi and Si(Cl)Me$_3$ to a solution of ArP=CCl$_2$). After 10 min, a solution of 9-fluorenone (417.6 mg) in 5 ml THF was added to the reaction mixture. Then the solution was kept at 30 °C for 4 h. After evaporation of the solvent, the compound was purified by chromatography on a SiO_2 column with a pentane–ether (9:1) mixture as an eluant. Colorless crystals of **2** were obtained from recrystallization in a hexane–ether mixture (m.p. 172 °C).

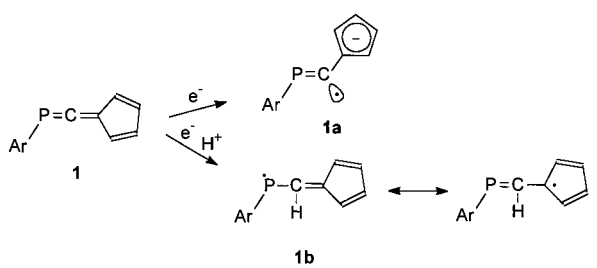

Scheme 2.

The synthesis of **2**(^{13}C) was carried out by following the same procedure, but by using ArP=^{13}CCl$_2$ as a reactant. This ^{13}C-enriched compound was obtained by reacting ArPCl$_2$ with ^{13}C(H)Cl$_3$ in presence of ^{n}BuLi as described by Goede and Bickelhaupt [12].

2.2. Analytical data

^{31}P-, ^{13}C-, ^{1}H-NMR spectra were recorded on a Bruker AC-200F (81 MHz), a Bruker Gemini 200 (50.2 MHz) and a Bruker 500DRX (500 MHz) spectrometer, respectively.

^{31}P{^{1}H}-NMR (CDCl$_3$, external H$_3$PO$_4$ used as reference), δ 90.2 ppm.

^{13}C-NMR (CDCl$_3$): δ 31.28 (s, Ar *para*-^{t}Bu CH$_3$), 33.91 (d, *ortho*-^{t}Bu CH$_3$, $^4J = 6.81$ Hz), 34.97 (s, C$_{25}$), 38.29 (s, C$_{21,29}$), 119.97 (s, C$_{6,9}$), 122.5 (d, C$_{17,19}$, $^3J = 1.71$ Hz), 123.38 (d, C$_1$, $^1J = 4.37$ Hz), 125.31 (s, C$_{3,12}$), 126.92 (s, C$_{4,11}$), 128.35 (s, C$_{5,10}$), 128.31 (d, C$_{15}$, $^1J = 70.3$ Hz), 138.53 (d, C$_{2,13}$, $^3J = 12$ Hz), 138.66 (d, C$_{7,8}$, $^4J = 4.32$ Hz), 150.30 (s, C$_{18}$), 154.29 (d, C$_{16,20}$, $^2J = 4.52$ Hz), 233.44 (d, C$_{14}$, $^1J_{C-P} = 20.4$ Hz).

^{1}H-NMR (CDCl$_3$): δ 1.31 (s, 9H, Ar *para*-^{t}Bu), 1.79 (s, 18H, Ar *ortho*-^{t}Bu), 7.26 (t, 2H, H$_{4,11}$ or H$_{5,10}$), 7.32 (t, 2H, H$_{5,10}$ or H$_{4,11}$), 7.46 (d, 2H, Ar–H, $^4J_{H-P} = 1.8$ Hz), 7.67 (d, 2H, H$_{6,9}$ or H$_{3,12}$), 7.69 (d, 2H, H$_{3,12}$ or H$_{6,9}$).

2.3. Crystal structure determination of **2**

$C_{32}H_{37}P$, $M_r = 452.6$, $\mu = 1.04$ mm^{-1}, monoclinic, $P2_1/n$, $Z = 4$, $a = 10.0842(5)$, $b = 20.364(3)$, $c = 13.381(2)$ Å, $\beta = 107.968(5)°$, $V = 2613.8(6)$ Å^3, colorless prism $0.20 \times 0.22 \times 0.28$ mm. Cell dimensions and intensities were measured at 200 K on a Stoe STADI4 diffractometer with graphite-monochromated Cu–K$_\alpha$ radiation ($\lambda = 1.5418$ Å). A total of 3367 measured

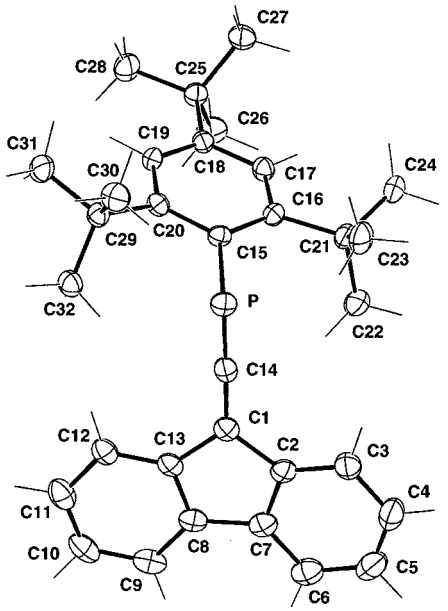

Fig. 1. Perspective view of the crystal structure of **2**, with atomic numbering. Ellipsoids are represented with 40% probability. P–C14 = 1.627(3), P–C15 = 1.865(2), C14–C1 = 1.336(4), C14–P–C15 = 104.8(1)°, C1–C14–P = 169.9(2), C13–C1–C14–P = 94(2)°, C15–P–C14–C1 = −172(2)°, C14–P–C15–C16 = −75.8(2).

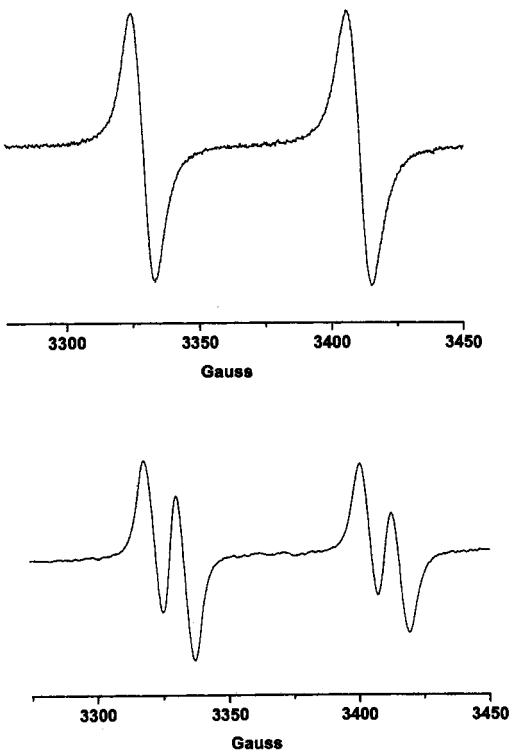

Fig. 2. EPR spectrum obtained at 300 K after electrochemical reduction of a solution of: (top) **2** in THF ($\nu_{klystron} = 9.451$ GHz) and (bottom) **2**(^{13}C) in THF ($\nu_{klystron} = 9.462$ GHz).

reflections, 3206 unique reflections of which 2572 were observables ($|F_o| > 4\sigma(F_o)$) were collected; R_{int} for equivalent reflections 0.032. Data were corrected for Lorentz and polarization effects and for absorption (min/max $T = 0.69234$, 0.83658). Full-matrix least-squares refinement based on F using weight of $1/[\sigma^2(F_o) + 0.0002(F^2)]$ gave final values $R = \omega R = 0.042$ and $S = 1.63(2)$ for 410 variables and 2572 contributing reflections. Hydrogen atoms were observed and refined with a fixed value of isotropic displacement parameters ($U = 0.05$ Å^2).

2.4. Cyclic voltammetry and EPR experiments

Voltammograms were recorded on a BAS station using a platinum electrode and an SCE reference electrode. Freshly distilled THF was used as a solvent and Bu_4NPF_6 (0.2 M) as an electrolyte. EPR measurements were carried out in a Bruker 200-D EPR spectrometer (100 KHz field modulation) equipped with a variable temperature attachment. Direct electrolysis of degassed solutions of **2** in THF (Bu_4NPF_6 as an electrolyte) was performed by using a quartz cell, a potentiometer and two platinum electrodes.

2.5. Calculations

The DFT calculations were performed with GAUSSIAN-98 [13]; CI treatments were carried out with the MELDF package [14]. Representations of the molecular structures and molecular orbitals were carried out with the MOLEKEL program [15].

3. Results

3.1. Experimental results

An ORTEP representation [16] of **2** is given in Fig. 1 together with principal geometrical parameters. The molecule is slightly bent (PCC = 169.9(2)°). The atoms C_1, C_{14}, P, C_{15} are almost coplanar (C_1–C_{14}–P–C_{15} = 172°). The corresponding plane is almost perpendicular (80.6(1)°) to the fluorene ring and makes a dihedral angle of 76.9(1)° with the Ar ring.

The cyclic voltammogram is characterized by an irreversible reduction wave at −1698 mV. Although a solution of **2** in THF or DME turns violet when in contact with a potassium mirror at 200 K, no EPR signal could be observed. When electrolyzed, a solution of **2** in THF turns deep red. As shown in Fig. 2a, electrochemical reduction, directly in the EPR cavity, leads to an EPR spectrum which is characterized by a large hyperfine splitting of 230 MHz. Probably due to the diffusion process around the electrode, this spectrum could be observed only after the electrolysis was stopped. Several attempts were made to detect additional hyperfine structure, however, even by using a

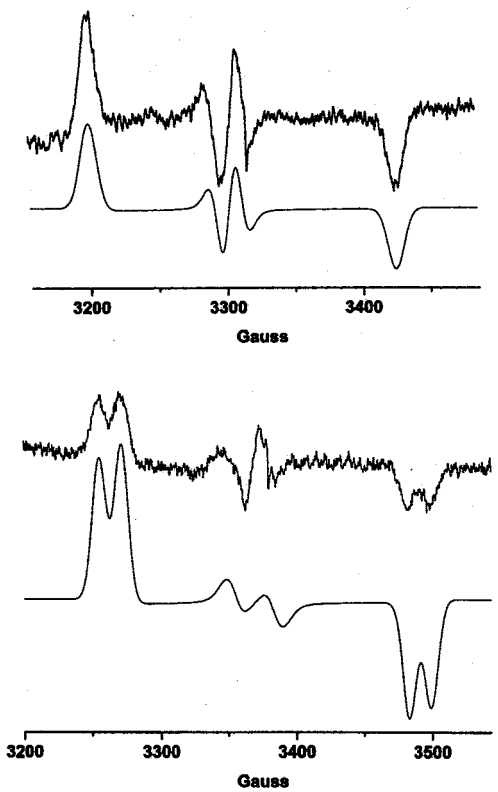

Fig. 3. Simulation and EPR spectrum obtained at 77 K after electrochemical reduction of a solution of: (top) **2** in THF ($\nu_{klystron} = 9.278$ GHz); (bottom) **2**(^{13}C) in THF ($\nu_{klystron} = 9.462$ GHz).

very small modulation amplitude, no other splitting could be resolved. A ^{13}C coupling of 33 MHz was clearly observed after reduction of the isotopically enriched phosphaallene (Fig. 2b). The frozen solution spectrum obtained at 77 K exhibits a particularly large hyperfine splitting, consistent with an anisotropic ^{31}P coupling tensor of axial symmetry (Fig. 3a). With the ^{13}C enriched compound, these external signals are split by a carbon coupling of 45 MHz (Fig. 3b). Simulation of the frozen solution spectra was carried out by retaining only the tensors which lead to the isotropic coupling constants observed with the liquid sample. These experimental tensors are given in Table 1.

3.2. Calculations

3.2.1. Computational background

The size of the molecules considered in our experiments is far too large to expect quantitative results from the available nonempirical methods. According to our experience from preceding studies of phosphorous compounds containing allenic fragments, replacement of bulky aryl groups by hydrogens provides suitable models while retaining the essential characteristics of the actual system. Density functional theory (DFT) and ab initio post-Hartree–Fock calculations were therefore performed on the model molecules **3**, $[\mathbf{3}]^{\bullet -}$ and $[\mathbf{3_H}]^{\bullet}$.

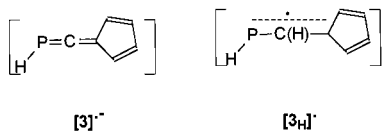

$[\mathbf{3}]^{\bullet -}$ $[\mathbf{3_H}]^{\bullet}$

The DFT calculations used the hybrid B3LYP method, with Becke's three-parameter nonlocal exchange potential [17] coupled to the nonlocal correlation functional of Lee et al. [18]; the basis set employed for the neutral closed-shell phosphaallene, namely, 6-311G**, was extended with diffuse functions to 6-311 + + G** in order to better describe the region, far from the nuclei, covered by the unpaired electron in the open-shell systems $[\mathbf{3}]^{\bullet -}$ and $[\mathbf{3_H}]^{\bullet}$. Vibrational frequencies have been calculated for the characterization of the energy minima and evaluation of zero-point energy corrections. These DFT calculations were aimed at determining the structure of the different systems. Due to their ability to describe spatial spin correlation, the DFT calculations were directly used for an evaluation of the anisotropic tensors of the radicals whereas CI calculations were necessary for a correct determination of the isotropic coupling constants. These latter calculations employed a basis of spin-adapted configuration in order to avoid spin contamination artifacts which, if marginal for the anisotropic parameters, may severely impede the determination of the isotropic values. The single-CI method coupled with the well-balanced 6-31 + G* basis set, which is known to give reliable

Table 1
EPR parameters measured after electrochemical reduction of a solution of **2** or **2**(^{13}C) in THF

	g		^{31}P hyperfine coupling [a] (MHz)		^{13}C hyperfine coupling [a] (MHz)	
	Liquid	Frozen solution	Liquid	Frozen solution	Liquid	Frozen solution
2	2.006	$g_\perp$ [b] = 2.008 $g_\parallel$ = 2.002	230.5	$T_\perp$ [b] = 30 $T_\parallel$ = 633		
2(^{13}C)	2.006	$g_\perp$ [b] = 2.007 $g_\parallel$ = 2.002	230.7	$T_\perp$ [b] = 28 $T_\parallel$ = 637	33	$T_\perp$ [b] = 27 $T_\parallel$ = 45

[a] Only the absolute value of the hyperfine coupling is determined from the EPR spectra.
[b] The perpendicular component was deduced from the isotropic (liquid solution) and the 'parallel' (frozen solution) values.

Table 2
Selected optimized parameters [a] of diamagnetic phosphaallenes and related experimental data

	Calculated data		Experimental data		
	3	$HP{=}C{=}CH_2$	**2** [b]		$ArP{=}C{=}CPh_2$
$P{=}C_1$	1.640	1.646	1.627	($P{=}C_{14}$)	1.625
$C_1{-}C_2$	1.319	1.304	1.336	($C_1{=}C_{14}$)	1.327
P–H	1.433	1.432			
$C_2{-}C_3$	1.477		1.486	($C_1{-}C_2$)	
$C_2{-}C_6$	1.477		1.478	($C_1{-}C_{13}$)	
$C_3{-}C_4$	1.352		1.404	($C_2{-}C_7$)	
$C_5{-}C_6$	1.352		1.402	($C_8{-}C_{13}$)	
$C_4{-}C_5$	1.470		1.462	($C_7{-}C_8$)	
$<PC_1C_2$	173.38	173.84	169.9	($P{-}C_{14}{-}C_1$)	167.7
$<HPC_1$	95.91		104.8	($C_{15}{-}P{-}C_{14}$)	
$<C_1C_2C_3$	126.79		127.7	($C_{14}{-}C_1{-}C_2$)	
$<C_2C_3C_4$	107.44		108.5	($C_1{-}C_2{-}C_7$)	
HPC_1C_2	180.00		172.2	($C_{15}{-}P{-}C_{14}{-}C_1$)	
$PC_1C_2C_3$	90.66	91.60 [c]	92.2	($P{-}C_{14}{-}C_1{-}C_2$)	91.50
$C_1C_2C_3C_4$	178.96		170.3	($C_{14}{-}C_1{-}C_2{-}C_7$)	

[a] Bond lengths in Å; bond and torsion angles in degrees. The calculated data for $HP{=}C{=}CH_2$ are obtained from Ref. [7], the experimental data for $ArP{=}C{=}CPh_2$ are obtained from the crystal structure [19].
[b] In parentheses: numbering in accordance with Fig. 1.
[c] Dihedral angle $PC_1C_2H_4$.

results for magnetic properties governed by spin-polarization effects, was used for that purpose. Finally, for sake of comparison, the dipolar hyperfine tensors and the isotropic couplings were estimated from the single-CI method and DFT, respectively.

3.2.2. The structure of the diamagnetic molecule

The C_s geometry (Table 2) found for **3** is close to that of $HP{=}C{=}CH_2$ [7] and typical of allenic compounds with the PH bond in a plane perpendicular to the Cp or CH_2 plane (Fig. 4).

The difference from allene comes from the replacement of a terminal CH_2 by a PH group which induces a slight bending of the allenic P=C=C fragment by $\sim 5°$. The P=C double bond is similar in both model compounds; the C=C allenic bond is a little shorter for a terminal CH_2 group than when the terminal carbon is part of the Cp ring. The comparison of the optimized parameters with those deduced from X-ray diffraction experiments on the bulky phosphaallenes shows the validity of the models (for $ArP{=}C{=}CPh_2$ see Ref. [19]. The fact that the allenic chain is slightly more bent ($\sim 5°$) and the RPC angle larger ($\sim 5°$) in the crystal structures is presumably a consequence of steric repulsion.

3.3. The structure of the paramagnetic species

As mentioned above, two radical species have to be considered for interpreting the EPR spectra. One is the negative ion, $[\mathbf{3}]^{\bullet -}$, where the electron is added in the antibonding π^* of the allenic group, the other is the neutral system obtained by protonation of the previous ion, $[\mathbf{3_H}]^{\bullet}$. The structural parameters, as obtained including exchange and correlation effects at the B3LYP level of theory, are reported in Table 3 together with the corresponding values of the $HP{=}C{=}CH_2$ derivatives [6] and illustrated in Fig. 5a.

Contrary to $[HP{=}C{=}CH_2]^{\bullet -}$ where two minimum energy structures were found ($[\mathbf{4_a}]^{\bullet -}$ and $[\mathbf{4_b}]^{\bullet -}$), only one stable conformation (Fig. 5a) was identified on the potential surface of $[\mathbf{3}]^{\bullet -}$.

$[\mathbf{4_a}]^{\bullet -}$ $[\mathbf{4_b}]^{\bullet -}$

It is clear that this conformation is similar to the $[\mathbf{4_a}]^{\bullet -}$ structure and that the $[\mathbf{4_b}]^{\bullet -}$ type geometry is not stable because of the steric repulsion with the neighboring hydrogen on the Cp ring.

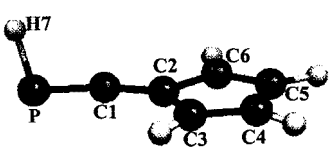

Fig. 4. DFT optimized structure of **3**.

Table 3
Selected optimized parameters [a] of paramagnetic phosphaallenes derivatives [b]

	$[3]^{\bullet -}$	$HP{=}C{=}CH_2^-$ $[4_a]^{\bullet -}$	$[3_{Ha}]^{\bullet}$	$HP^{\bullet}$–CH=CH_2 conformer **a**	$[3_{Hb}]^{\bullet}$	$HP^{\bullet}$–CH=CH_2 conformer **b**
$P{=}C_1$	1.685	1.740	1.755	1.785	1.749	1.781
C_1–C_2	1.377	1.335	1.319	1.354	1.319	1.355
P–H	1.433	1.438	1.427	1.427	1.427	1.430
C_2–C_3	1.453		1.470		1.468	
C_2–C_6	1.450		1.457		1.460	
C_3–C_4	1.381		1.354		1.355	
C_5–C_6	1.382		1.360		1.359	
C_4–C_5	1.441		1.475		1.475	
$<PC_1C_2$	146.70	140.31	124.19	122.20	131.23	127.73
$<HPC_1$	99.04		95.77		97.68	
$<C_1C_2C_3$	127.71		127.99		129.15	
$<C_2C_3C_4$	108.47		107.73		107.75	
Di-HPC_1C_2	15.81		0.0	0.0	180.0	180.0
Di-$PC_1C_2C_3$	29.48	18.32 [c]	0.0	0.0 [c]	0.0	0.0 [c]
Di-$C_1C_2C_3C_4$	178.55		0.0	0.0	0.0	0.0

[a] Bond lengths in Å; bond and torsion angles in degrees.
[b] The data for $HP{=}C{=}CH_2^-$ and $HP^{\bullet}$–CH=CH_2 are obtained from Ref. [7].
[c] Dihedral angle $PC_1C_2H_4$.

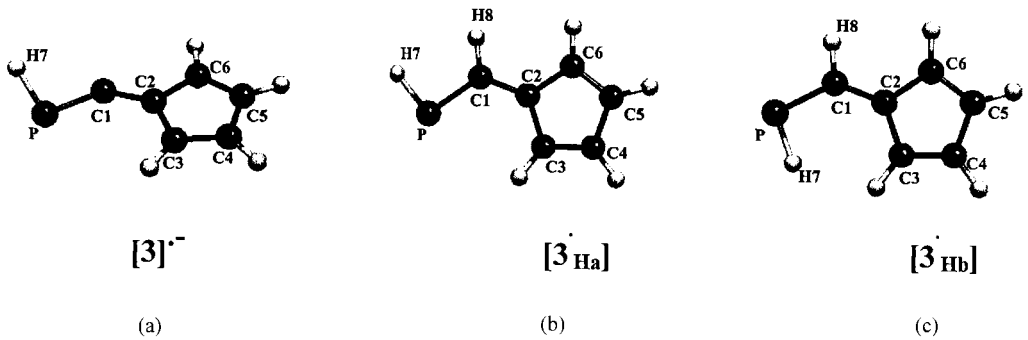

Fig. 5. DFT optimized structures of: (a) $[3]^{\bullet -}$; (b) $[3_{Ha}]^{\bullet}$; (c) $[3_{Hb}]^{\bullet}$.

The presence of the Cp ring accommodates the negative charge which leads to a substantial lengthening (~ 0.05 Å) of the CC bond compared to the simplest phosphaallenic anion. With respect to the neutral parent, one can remark the expected increase in the bond lengths after the addition of an electron in an antibonding level; the most significant change occurs for the CC bond due to the transition from a neutral fulvenic to cyclopentadienide structure. Simultaneously, one observes a closing of the PCC angle by $\sim 25°$.

Concerning the neutral species $[3_H]^{\bullet}$ obtained after protonation of the negative ion, we identified two isomers ($[3_{Ha}]^{\bullet}$ and $[3_{Hb}]^{\bullet}$) of allylic structure as previously obtained for $HP^{\bullet}$–CH=CH_2. They are planar (Fig. 5b and c) and very close in energy (0.4 kcal mol^{-1}), both corresponding to $^2A''$ electronic configurations. In view of the size of the Ar substituent, only the minimum $[3_{Ha}]^{\bullet}$ of the model radical is significant for our purpose. The P=C=C backbone is bent $\sim 125°$ in agreement with the allylic structure but contrary to $HP^{\bullet}$–CH=CH_2 the CC bond is now shorter than in the anion because of the stabilization provided by the fulvenic structure.

4. Discussion

In order to compare the experimental results with the quantum mechanical predictions, the EPR hyperfine couplings have been decomposed into isotropic and anisotropic components. These values were obtained by assuming that the three eigenvalues of each tensor have the same sign.

The comparison between the experimental couplings and the atomic coupling constants [20] ($A^*_{iso}(^{31}P) = 13\,360$ MHz, $\tau^*_{aniso}(^{31}P) = 733$ MHz, $A^*_{iso}(^{13}C) = 3777$ MHz, $\tau^*_{iso}(^{13}C) = 214$ MHz) indicates that ca. 55% of the spin is localized in a phosphorus p orbital while only ($\mp$)5% is localized in the central carbon p-orbital. The mutual orientation of the experimental tensors indicates that these atomic p orbitals are parallel. The contributions of the carbon and phosphorus s orbitals

appear to be very small ($\rho_s(P) = 0.017$, $\rho_s(C) = 0.009$) and probably due to inner shell spin polarization.

As shown above, comparison between the crystal structure of **2** and the optimized geometry of **3** indicates that the DFT calculations are appropriate for predicting the structural properties of the P=C=Cp group. The natural approach in the identification of a transient paramagnetic species is to first ascertain the electronic state which means the type of radical. The task is greatly simplified when anisotropic values of the hyperfine couplings can be obtained from single crystal or frozen solution EPR experiments. In this case, this can be done most of the time by careful examination of the hyperfine anisotropic tensors and their symmetry. From a theoretical point of view, these tensors can be apprehended by examination of the spatial distribution of the spin density. This is illustrated in Fig. 6 where 3D views of the total spin density have been reported for the negative ion (Fig. 6a) and the most probable allylic isomers (Fig. 6b and c).

The two species are obviously different. The negative ion has most of its spin density located on the central carbon of the phosphaallenic backbone showing a σ character while the phosphaallylic radical of $^2A''$ symmetry has a small negative spin density on this same carbon and the major part distributed between phosphorus and the carbons of the Cp ring. The corresponding values of the anisotropic tensors obtained both at the B3LYP/6-311 + + G** and at the SCI levels are given in Table 5.

A cursory view of the DFT results shows that difference already visible on the spatial distribution of the spin density is numerically confirmed with a coupling for the central carbon much larger in the negative ion than in the allylic radical. Moreover, in $[\mathbf{3}]^{\bullet -}$ the principal directions $\tau_{\parallel}(^{13}C)$ and $\tau_{\parallel}(^{31}P)$ make an angle of 52°, whereas, in $[\mathbf{3_H}]^{\bullet}$, these two directions are aligned along the normal to the PCC plane.

The experimental phosphorus and carbon anisotropic couplings are in good agreement with the DFT values

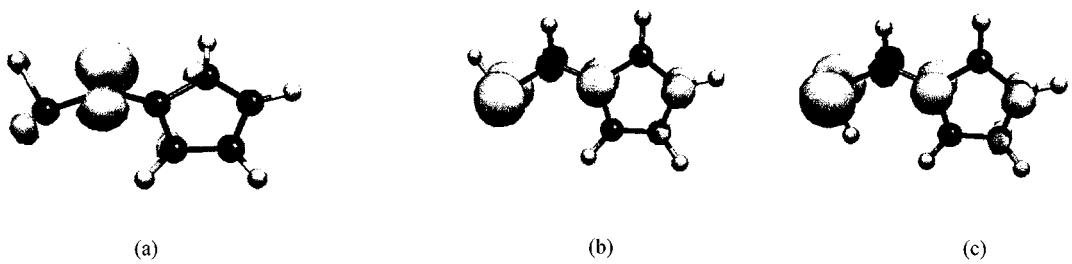

(a) (b) (c)

Fig. 6. Representation of the SOMO for: (a) $[\mathbf{3}]^{\bullet -}$; (b) $[\mathbf{3_{Ha}}]^{\bullet}$; (c) $[\mathbf{3_{Hb}}]^{\bullet}$.

Table 4
Experimental isotropic and anisotropic coupling constants (MHz) obtained after reduction of a solution of **2** or **2**(^{13}C)

^{31}P coupling			^{13}C coupling		
A_{iso}	τ_{aniso}		A_{iso}	τ_{aniso}	
(±)230.6	$\tau_{\parallel} = (\pm)402.4$	$\tau_{\perp} = (\mp)201.2$	(∓)33	$\tau_{\parallel} = (\mp)12$	$\tau_{\perp} = (\pm)6$

Table 5
Anisotropic coupling constants (MHz) of reduction products of phosphaallenes

	$\mathbf{3}^{\bullet -}$		$[\mathbf{3_{Ha}}]^{\bullet}$		$[\mathbf{3_{Hb}}]^{\bullet}$	
	DFT	SCI	DFT	SCI	DFT	SCI
τ ^{31}P	−52	−74	−225	−176	−222	−190
	−49	−68	−210	−194	−208	−173
	101	142	435	370	430	363
τ ^{13}C	−54	−41	11	10	11	11
	−53	−36	14	7	15	7
	107	78	−25	−17	−26	−18
τ ^{1}H			−2	−3	−2	−3
			−3	−2	−3	−3
			5	5	5	6

calculated for $[\mathbf{3_H}]^{\bullet}$ shown in Table 4. The calculated proton coupling is small and was not resolved on the EPR spectrum. DFT results provide, therefore, clear-cut evidence that the EPR spectra recorded after reduction of **2** is due to $[\mathbf{2_H}]^{\bullet}$ and cannot be attributed to the negative ion $[\mathbf{2}]^{\bullet -}$. As shown in Table 5, although the anisotropic values calculated by CI slightly differ from those calculated by DFT, they all exhibit the same feature: by passing from $[\mathbf{3}]^{\bullet -}$ to $[\mathbf{3_H}]^{\bullet}$, ^{31}P-$\tau_{\parallel}$ drastically increases while the absolute value of ^{13}C-$\tau_{\parallel}$ decreases.

The isotropic values ($\sim$160 MHz for ^{31}P and $\sim -$34 MHz for ^{13}C) calculated at the SCI level for $[\mathbf{3_H}]^{\bullet}$ are consistent with the experimental spectra. The value found for ^{1}H ($\sim$6 MHz) is small, and explains why it could not be resolved on the EPR spectrum. On the other hand, the values calculated for $[\mathbf{3}]^{\bullet -}$ (18 MHz for ^{31}P and 98 MHz for ^{13}C) totally disagree with the experimental values and confirm that the reduction product of **2** observed by EPR is the phosphaallylic radical $\mathbf{2_H}^{\bullet}$ and not the radical anion $[\mathbf{2}]^{\bullet -}$. It is worthwhile remarking that the DFT isotropic values (for $[\mathbf{3_{Ha}}]^{\bullet}$ ^{31}P: 85 MHz, ^{13}C: -29 MHz, for $[\mathbf{3_{Hb}}]^{\bullet}$ ^{31}P: 84 MHz, ^{13}C: -30 MHz) lead to the same conclusion, although the ^{31}P value is appreciably smaller than the CI estimation.

The isotropic and anisotropic coupling constants measured in the present study are similar with those previously reported for $[ArP–CH=CPh_2]^{\bullet}$ detected after reduction of $ArP=C=CPh_2$. This is quite consistent with the protonation of the radical anion and shows that the presence of the cyclopentadienyl ring does not considerably affect the spin distribution of the phosphaallylic radical.

5. Concluding remarks

DFT calculations of the dipolar coupling and CI calculations of the isotropic hyperfine couplings lead to a clear differentiation between the radical anion $[\mathbf{3}]^{\bullet -}$ and the phosphaallylic radical $[\mathbf{3_H}]^{\bullet}$. They show that, even when the terminal carbon of the –P=C=C system is incorporated in a cyclopentadienyl ring (e.g. **2**), the EPR spectrum obtained after reduction of the phosphaallene is not due to the anion (e.g. $[\mathbf{2}]^{\bullet -}$) but to the corresponding phosphaallylic radical (e.g. $[\mathbf{2_H}]^{\bullet}$). These results confirm the strong basic character of phosphaallenic radical anions.

6. Supplementary material

Crystallographic data for the structural analysis have been deposited with the Cambridge Crystallographic Data Centre, CCDC no. 162742 for compound **2**. Copies of this information may be obtained free of charge from The Director, CCDC, 12 Union Road, Cambridge CB2 1EZ, UK (Fax: +44-1223-336033; e-mail: deposit@ccdc.cam.ac.uk or www: http://www.ccdc.cam.ac.uk).

Acknowledgements

We thank the Swiss National Science Foundation for financial support. Calculations were performed at the Swiss Center for Scientific Computing.

References

[1] Y. Canac, D. Bourissou, A. Baceiredo, H. Gornitzka, W.W. Schoeller, G. Bertrand, Science 279 (1998) 2080.
[2] (a) M. Geoffroy, A. Jouaiti, G. Terron, M. Cattani-Lorente, Y. Ellinger, J. Phys. Chem. 96 (1992) 8241;
(b) A. Jouaiti, A. Al Badri, M. Geoffroy, G. Bernardinelli, J. Organomet. Chem. 529 (1997) 143.
[3] (a) B. Cetinkaya, A. Hudson, M. Lappert, H. Goldwhite, J. Chem. Soc. Chem. Commun. (1982) 609;
(b) M. Culcasi, G. Gronchi, J. Escudié, C. Couret, L. Pujol, P. Tordo, J. Am. Chem. Soc. 108 (1986) 3130;
(c) S. Shah, S.C. Burdette, S. Swavey, F.L. Urbach, J.D. Protasiewicz, Organometallics 16 (1997) 3395;
(d) S. Loss, A. Magistrato, L. Cataldo, S. Hoffmann, M. Geoffroy, U. Röthlishberger, H. Grützmacher, Angew. Chem. Int. Ed. Engl. 40 (2001) 723.
[4] (a) J. Escudié, H. Ranaivonjatovo, L. Rigon, Chem. Rev. 100 (2000) 3639;
(b) L. Rigon, H. Ranaivonjatovo, J. Escudié, A. Dubourg, J.-P. Declercq, Chem. Eur. J. 5 (1999) 774.
[5] H. Sidorenkova, M. Chentit, A. Jouaiti, G. Terron, M. Geoffroy, Y. Ellinger, J. Chem. Soc. Perkin Trans. 2 (1998) 71.
[6] (a) A. Alberti, M. Benaglia, M. D'Angelantonia, S.S. Emmi, M. Guerra, A. Hudson, D. Macciantelli, F. Paolucci, S. Roffia, J. Chem. Soc. Perkin Trans. 2 (1999) 309;
(b) A. Alberti, M. Benaglia, M. Cuerra, A. Hudson, J. Macciantelli, J. Chem. Soc. Perkin Trans. 2 (1999) 1567.
[7] M. Chentit, H. Sidorenkova, M. Geoffroy, Y. Ellinger, J. Phys. Chem. A 102 (1998) 10469.
[8] (a) K.B. Dillon, F. Mathey, J.F. Nixon, Phosphorus: the Carbon Copy, Chichester, Wiley, 1998;
(b) in: M. Regitz, O.J. Scherrer (Eds.), Multiple Bonds and Low Coordination in Phosphorus Chemistry, Thieme, Stuttgart, 1999, p. 1999.
[9] M. Yoshifuji, J. Organomet. Chem. 611 (2000) 210.
[10] A. Al Badri, M. Chentit, M. Geoffroy, A. Jouaiti, J. Chem. Soc. Faraday Trans. 93 (1997) 3631.
[11] M. Yoshifuji, S. Sasaki, N. Inamoto, Tetrahedron Lett. 30 (1989) 839.
[12] S.J. Goede, F. Bickelhaupt, Chem. Ber. 124 (1991) 2677.
[13] M.J. Frisch, G.W. Trucks, H.B. Schlegel, G.E. Scuseria, M.A. Robb, J.R. Cheeseman, V.G. Zakrzewski, J.A. Montgomery, R.E. Stratmann, J.C. Burant, S. Dapprich, J.M. Millam, A.D. Daniels, K.N. Kudin, M.C. Strain, O. Farkas, J. Tomasi, V. Barone, M. Cossi, R. Cammi, B. Mennucci, C. Pomelli, C. Adamo, S. Clifford, J. Ochterski, G.A. Petersson, P.Y. Ayala, Q. Cui, K. Morokuma, D.K. Malick, A.D. Rabuck, K. Raghavachari, J.B. Foresman, J. Cioslowski, J.V. Ortiz, B.B. Stefanov, G. Liu, A. Liashenko, P. Piskorz, I. Komaromi, R. Gomperts, R.L Martin, D.J. Fox, T. Keith, M.A. Al-Laham,

C.Y. Peng, A. Nanayakkara, C. Gonzalez, M. Challacombe, P.M.W. Gill, B.G. Johnson, W. Chen, M.W. Wong, J.L. Andres, M. Head-Gordon, E.S. Replogle, J.A. Pople, GAUSSIAN-98 (Revision A.7), Gaussian, Inc., Pittsburgh PA, 1998.

[14] L. McMurchie, S. Elbert, E.R. Davidson. (modified by D. Feller, R.J. Cave, D. Rawlings, R. Frey, R. Daasch, L. Nitzche, P. Phillips, K. Iberle, C. Jackels, E.R. Davidson, MELDF Suite of Programs, 1990/91.

[15] P. Flukiger, PhD Thesis no. 2561, 1992.

[16] L.J. Farrugia, ORTEP-3 Program, Department of Chemistry; University of Glasgow, 1997.

[17] A.D. Becke, Phys. Rev. A. 38 (1988) 3098.

[18] C. Lee, W. Yang, R.G. Parr, Phys. Rev. B 54 (1988) 785.

[19] R. Appel, P. Fölling, B. Josten, M. Siray, V. Winkhaus, F. Knoch, Angew. Chem. Int. Ed. Engl. 23 (1984) 619.

[20] J.R. Morton, K.F. Preston, J. Magn. Reson. 30 (1978) 577.